Interlayer exchange coupling between FeCo and Co ultrathin films through Rh(001) spacers

S. Blizak,[1,*] G. Bihlmayer,[2,†] S. Blügel,[2] and S. E. H. Abaidia[1]

[1]*Unité de Recherche Matériaux Procédés et Environnement (URMPE), University M'Hamed Bougara of Boumerdés (UMBB), 35000 Boumerdés, Algeria*

[2]*Peter Grünberg Institut and Institute for Advanced Simulation, Forschungszentrum Jülich and JARA, 52425 Jülich, Germany*

(Received 9 September 2014; revised manuscript received 10 November 2014; published 9 January 2015)

Using spin density functional theory (SDFT) calculations, we have studied the magnetic states, including collinear and noncollinear magnetic interlayer coupling, of $Fe_{1-x}Co_x$ ultrathin films sandwiching Rh(001) layers. We found very large values for the interlayer exchange coupling (IEC) in $Co/Rh_n/Co$ or $(FeCo)_m/Rh_n/Co$ structures as compared to, e.g., Ag or Au spacer layers. The IEC oscillates with the Rh spacer thickness showing a transition between strong antiferromagnetic and ferromagnetic coupling between five- and seven-layer thickness of the Rh film. Moreover, depending on the thickness of the FeCo film, a reorientation transition between in-plane and out-of-plane easy axis was found when spin-orbit coupling is considered in the calculations. This result suggests that, for specific arrangements such as $(FeCo)_2/Rh_5/Co$ structures, a competition between IEC and magnetic anisotropy of coupled films may result in noncollinear ordering. This possibility was studied with constrained, noncollinear SDFT calculations and the results were mapped onto a classical spin model to explore the richness of spin structures that can arise in these multilayer systems.

DOI: 10.1103/PhysRevB.91.014408 PACS number(s): 75.70.Ak, 71.15.Mb, 73.20.−r

I. INTRODUCTION

The interlayer exchange coupling (IEC) between ferromagnetic (FM) transition-metal layers separated by a nonmagnetic metal spacer has been intensively investigated, both experimentally and theoretically: It was first observed in 1986 for Dy and Gd films separated by Y interlayers and for Fe films separated by Cr interlayers [1–3]. In 1988, the discovery of the giant magnetoresistance (GMR) effect in the Fe/Cr system led to enhanced interest in the magnetic coupling in multilayers of transition-metal ferromagnets due to a variety of applications of this effect. Further, it was established that the oscillation between ferromagnetic and antiferromagnetic (AFM) magnetic coupling, as a function of interlayer thickness, is a general phenomenon of transition-metal ferromagnets separated by nonmagnetic interlayers [4,5]. The oscillatory coupling behavior has been described with several models, e.g., the RKKY-type model and the quantum well model [6,7]. The presence of biquadratic exchange coupling was observed at the same time by Heinrich *et al.* [8] on Co/Cu/Co(001) and by Rührig *et al.* [9] in Fe/Cr/Fe(001). Slonczewski reviewed theories of the IEC, in particular describing the fluctuations of spacer thickness and loose spin theory, which is to explain the biquadratic coupling phenomena [10]. Later reviews emphasized the role of biquadratic coupling [11] and bilinear coupling [12] for the oscillatory behavior of the IEC. A more general theoretical model, the quantum interference model, is given by Bruno [13] describing the IEC in terms of the quantum interferences due to the (spin-dependent) reflections of Bloch waves at the paramagnet-ferromagnet interfaces.

Materials with large magnetic moments and a strong perpendicular anisotropy are of great interest for information technology and recording media applications such as magnetic field sensors [14]. In recent research, a great deal of attention has been devoted to transition-metal (TM) alloy films on various substrates. In Ref. [15], Yildiz and collaborators studied tetragonally distorted $Fe_{1-x}Co_x$ alloy films on Rh(001) which show large magnetic moments and a strong perpendicular anisotropy in a wide thickness (up to 15 ML) and composition range ($0.4 < x < 0.6$) even at room temperature, while for large x in-plane magnetized films were observed. Also, multilayer structures of FeCo alloys have been studied experimentally [16,17]. It was established that IEC through Rh(001) has an important role determining whether the magnetic anisotropy of the whole system is finally in plane or out of plane. The Rh spacers are expected to mediate an exchange coupling between the adjacent magnetic films, which can orient their magnetizations either parallel or antiparallel, depending on the spacer thickness [3]. A competition between the interlayer coupling (which can be tuned by the Rh spacer thickness) with different easy axes in the two coupled films (which can be tuned by the film composition) offers a unique possibility to realize a nonorthogonal magnetization configuration of the two magnetic films, i.e., a noncollinear order due to magnetic anisotropy energy (MAE) and interlayer exchange coupling in these structures [17]. These findings motivate a more systematic investigation of the MAE and IEC in $Fe_{1-x}Co_x$ alloy films on a Rh(001) substrate.

In this paper, we investigate the role of the IEC and MAE in determining the desired magnetic properties of $Fe_{1-x}Co_x$ alloy layers on Rh(001)/Co, where the magnetization of the Co layer is assumed to be fixed in plane.[1] We compare the results to Co monolayers on Rh(001)/Co. In Sec. II, we outline the computational method, while in Sec. III, we study the main

*Present address: Peter Grünberg Institut and Institute for Advanced Simulation, Forschungszentrum Jülich and JARA, 52425 Jülich, Germany.

†g.bihlmayer@fz-juelich.de

[1]This simulates the experimental situation where eight-layer-thick Fe films were used to create a stable in-plane magnetization [17].

properties of FeCo and Co films on Rh(001), in particular the magnetic order, the magnetic moments, and the magnetic anisotropy. Fundamental aspects of IEC [without and with spin-orbit coupling (SOC) considered] are given in Sec. IV. We calculate the interlayer exchange coupling through Rh(001) for FeCo/Rh_n/Co and $(FeCo)_m$/Rh_5/Co films in Sec. V and finally conclude with a summary in Sec. VI.

II. COMPUTATIONAL DETAILS

The Co/Rh_n/Co, FeCo/Rh_n/Co, and $(FeCo)_2$/Rh_5/Co thin (001) oriented films were addressed to study their magnetic states including collinear and noncollinear magnetic coupling using spin density functional theory (SDFT) [18–20]. The FeCo layers were modeled in a checkerboard arrangement of the Fe and Co atoms, as this is energetically most favorable on a Rh(001) substrate [21]. All calculations in this work were made using the FLEUR [22] implementation of the all-electron full-potential linearized augmented plane-wave method [23] in film geometry [24]. The generalized gradient approximation to the exchange-correlation functional of Perdew *et al.* is used [25]. The noncollinear order was treated in the framework of the constrained SDFT [26]. Spin-orbit interactions were considered using the force theorem [27] and in a so-called second variational step with the scalar-relativistic eigenfunctions as a new, compacted basis [28]. In the case of self-consistent noncollinear calculations, the SOC term is directly included in the Hamiltonian. The films are modeled by a symmetric n-layer Rh(001) slab covered by $3d$ transition-metal monolayers (ML) on each side, using the calculated Rh in-plane lattice constant 3.819 Å [29] and relaxations as described in Sec. III. The augmented plane-wave cutoff parameter is chosen such that its product with the smallest muffin-tin radius is $k_{\max} R_{\min} = 9$.

III. SOME PROPERTIES OF FeCo AND Co FILMS ON Rh(001)

In low-dimensional magnetic structures, the ground-state properties are determined by the interactions of local spin and orbital moments of different size. These interactions play an important role in the formation of the magnetic order and the magnetic coupling at interfaces or across spacer layers. The spin-orbit coupling and dipole-dipole interactions sum up to the magnetic anisotropy energy, which couples the direction of the magnetization to the lattice and determines the easy and hard axes of the magnetization. We will give in this section the main properties of the FeCo and Co films, in particular we focus on the relaxations, the magnetic order, moments, and the magnetocrystalline anisotropy. These properties are summarized in Tables I and II.

The relaxations between the layers i and j are characterized by

$$\Delta d_{ij} = \frac{(d_{ij} - d_0)}{d_0}, \tag{1}$$

where d_{ij} is the spacing between the neighboring layers i and j, and d_0 is the ideal bulk interlayer distance of the substrate (1.91 Å). For the FeCo film, we observe a corrugation of the topmost layer, which is characterized by the difference of the vertical distance between Fe and Co atoms:

TABLE I. Relaxations of the first and second interlayer spacing on FeCo/Rh_n/Co film on the alloy (FeCo) side and on the Co-terminated surface.

	FeCo			Co	
n	Δd_{FeCo} (Å)	Δd_{12} (%)	Δd_{23} (%)	Δd_{12}(%)	Δd_{23}(%)
7	0.020	−10.65	2.00	−13.29	2.71
6	0.024	−10.59	1.98	−13.44	2.35
5	0.021	−10.61	2.28	−13.28	2.90
4	0.032	−11.08	2.58	−13.91	3.23
3	0.025	−10.52	1.33	−13.19	1.05
2	0.011	−11.21	1.88	−14.13	1.88

$\Delta d_{\mathrm{FeCo}} = (z_{\mathrm{Fe}} - z_{\mathrm{Co}})$. Δd_{ij} refers in this case to the average vertical distance of Fe and Co. Table I represents the relaxations of an FeCo/Rh_n/Co film as a function of the rhodium thickness in terms of the number of rhodium layers n. We note that the corrugation of the topmost layer and all relaxations Δd_{ij} are almost constant for $n \geqslant 5$ indicating that at this thickness, the structure of the two sides of the film can be considered as decoupled from each other.

In Ref. [21], we analyzed the magnetic order of the ground state of $Fe_{1-x}Co_x$ films by determining the total-energy difference between the in-plane AFM (or ferrimagnetic, FIM) and the FM configurations:

$$\Delta E = E_{\mathrm{AFM(FIM)}} - E_{\mathrm{FM}}. \tag{2}$$

Positive values indicate a FM ground state, while negative values denote in-plane AFM (FIM) order. To calculate this difference, 78 $\mathbf{k}_{\parallel}$ points in the irreducible Brillouin zone (IBZ) were used for the $c(2 \times 2)$ unit cells. We found a FM ground state for Co and FeCo, almost independent from the thickness of the Rh(001) spacer (see Table II and Ref. [21]). Also, a thicker $(FeCo)_2$ film with two FeCo layers is FM, all tested FIM structures were found to be higher in energy by at least 89.7 meV. The FM films show large averaged magnetic moments of about 2.5 and 2.0 μ_{B} per $3d$ TM atom for FeCo and Co films, respectively.

The magnetic anisotropy is one of the most important intrinsic quantities in the field of the magnetic thin films and multilayers. It allows us to determine the magnetization

TABLE II. The magnetocrystalline anisotropy MCA, spin magnetic moments m, and total-energy differences $\Delta E = (E_{\mathrm{AFM(FIM)}} - E_{\mathrm{FM}})$ per TM atom of cobalt and iron-cobalt alloys in ferromagnetic structure on n-layer rhodium (001) films. The data for $n = 7$ are taken from Ref. [21]. A positive value of the MCA indicates an easy axis perpendicular to the film plane.

TM	n	K_{MCA} (meV)	m_{Fe} (μ_{B})	m_{Co} (μ_{B})	$m_{\mathrm{Rh-I}}$ (μ_{B})	ΔE (meV)
Co	5	−0.53		2.03	0.43	160.0
	7	−0.09		2.03	0.48	161.2
FeCo	5	−0.03	3.08	1.89	0.31	87.3
	7	0.25	3.08	1.91	0.34	81.9
$(FeCo)_2$	5	0.11	2.96	1.86	0.31	89.7
			2.68	1.73	0.28	

direction [here, we compare the in-plane (100) to the out-of-plane (001) direction] of the magnetic system, and also to estimate its critical temperature in two dimensions. In principle, two terms contribute to the MAE: the dipole-dipole interaction, leading in a ferromagnetic film to an in-plane magnetic shape anisotropy (MSA) and the spin-orbit coupling term giving the dominant contribution to the magnetocrystalline anisotropy (MCA). The MCA arises from the anisotropy of the spin-orbit coupling interaction, i.e., it is the difference of total energies obtained from Hamiltonians including the spin-orbit coupling term with the magnetization pointing in two different directions. In the case of uniaxial anisotropy, the energy difference between the situations where a spin is perpendicular or parallel to the film normal, chosen to be $\hat{\mathbf{e}}_z$, is given by the anisotropy constant K_{MCA} (note that here the MCA is assumed to be isotropic in the film plane). Calculations of the magnetic anisotropy confirmed that FeCo layers on Rh(001) can have an out-of-plane easy axis in their ground state, while the magnetization of Co is generally in-plane oriented. Table II shows that, in contrast to the properties discussed above, the MCA of the films depends sensitively on the thickness of the Rh spacer: for five layers Rh(001) also the FeCo monolayer shows a (small) in-plane anisotropy, only the FeCo double layer has an out-of-plane easy axis.

The MSA is the consequence of the anisotropy of the dipole-dipole interaction. We obtain a value of 0.02 meV per atom for FeCo film, which is one order of magnitude smaller than the values obtained for the MCA [21].

IV. PHENOMENOLOGICAL DESCRIPTION

A. Interlayer exchange coupling (IEC)

Exchange coupling between magnetic layers across a nonmagnetic metal has been frequently observed in many layered systems of the type FM1/NM/FM2 where FM represents a ferromagnetic transition metal (Fe, Co, Ni, and most of their alloys), and NM is a noble metal (Cu, Ag, Au) or a nonmagnetic transition metal (Mo, Ru, Re, Ir, Rh, Y,...). The magnetic moments of the FM1 layer couple to those of the FM2 layer through the nonmagnetic metal spacer. This coupling originates from a polarization of the electrons of the nonmagnetic layer induced by contact with the magnetic layers. For ferromagnetic films such as Fe/Au/Fe and Fe/Cr/Fe, the IEC stabilizes either a collinear (parallel or antiparallel) or, less frequently, a noncollinear alignment of the magnetizations on opposite sides of the interlayer. The actual alignment is also affected by other factors such as the magnetic anisotropy or an applied external magnetic field $\mathbf{H}$. In order to take into account the possibility of noncollinear interlayer exchange coupling, it is convenient to introduce a phenomenological coupling energy of the form

$$\begin{aligned} E(\varphi) &= J_{\mathrm{BL}}\mathbf{e}_1 \cdot \mathbf{e}_2 + J_{\mathrm{BQ}}(\mathbf{e}_1 \cdot \mathbf{e}_2)^2 \\ &= J_{\mathrm{BL}} \cos\varphi + J_{\mathrm{BQ}} \cos^2\varphi, \end{aligned} \tag{3}$$

where $\mathbf{e}_1$, $\mathbf{e}_2$ are the magnetic moment directions of two magnetic layers separated by the nonmagnetic layer and φ is the angle between them. J_{BL} and J_{BQ} are the bilinear and biquadratic exchange coupling parameters, respectively. This expansion describes generalizations of the Heisenberg form of interlayer coupling energy. In the literature, various definitions of the coupling parameters are in use. Here, we use the form of the interlayer coupling energy introduced by Bruno [30,31]. If $J_{\mathrm{BQ}} = 0$, the oscillatory exchange coupling is simply described by an oscillation of J_{BL} between positive and negative values. If the term J_{BL} dominates, the coupling is AFM (FM) for positive (negative) J_{BL}. If the term J_{BQ} dominates and is positive, the energy is a minimum for $\varphi = \pm\pi/2$, so that 90° coupling is stable if $J_{\mathrm{BL}} = 0$. The origin of the two coupling coefficients is quite different: The bilinear term is closely related to the corresponding volume exchange stiffness effect and derivable from the same quantum mechanical foundations. In contrast, the origin of biquadratic exchange coupling can be either intrinsic due to the band properties of the nonferromagnetic spacer [32] or extrinsic due to interface roughness [33].

B. Spin-orbit coupling (SOC) effects

Spin-orbit coupling plays an important role in the formation of the magnetic structure via the MCA, which determines the easy axis in ultrathin magnetic films. This affects the actual alignment of the magnetizations on opposite sides of the spacer layer in interlayer exchange-coupled films. Assuming the magnetization direction on one side of the film to be fixed, one can consider the anisotropy of the opposite layer as a term K that can be added to the Heisenberg Hamiltonian

$$H = -\sum_{ij} J_{ij}\mathbf{S}_i \cdot \mathbf{S}_j + \sum_i \mathbf{S}_i \cdot \mathsf{K}_i \cdot \mathbf{S}_i, \tag{4}$$

where the tensor of single-site anisotropy constants K_i determines the strength of the anisotropy as well as the direction of minimal and maximal energy, named easy and hard axes, respectively. In model Hamiltonian calculations or Monte Carlo simulations, this type of Hamiltonian can be used when inclusion of an anisotropy term is required. Thus, the total energy including the additional biquadratic term and the uniaxial anisotropy, which represents the anisotropy of the spin-orbit coupling, can be expressed as follows:

$$E(\varphi) = J_{\mathrm{BL}} \cos\varphi + J_{\mathrm{BQ}} \cos^2\varphi + K_{\mathrm{MCA}}(\cos^2\varphi - 1). \tag{5}$$

Therefore, noncollinear spin arrangements can be expected if $2(J_{\mathrm{BQ}} + K_{\mathrm{MCA}}) > |J_{\mathrm{BL}}|$. With increasing spacer thickness, the IEC will decrease, but the anisotropy term in the expression converges to a constant (and, in our case, positive) value, i.e., we can expect that there is some Rh thickness, where this relation is fulfilled. In the following, we will determine the strength of these terms in FeCo films that are exchange coupled to a Co layer with fixed in-plane magnetization via Ru(001) spacer layers.

V. INTERLAYER EXCHANGE COUPLING THROUGH Rh(001)

A. FeCo/Rh$_n$/Co films

The bilinear contribution to IEC is calculated by taking the energy differences between antiparallel ($\uparrow\downarrow$) and parallel ($\uparrow\uparrow$) aligned magnetic thin films on the two sides of the Rh(001)

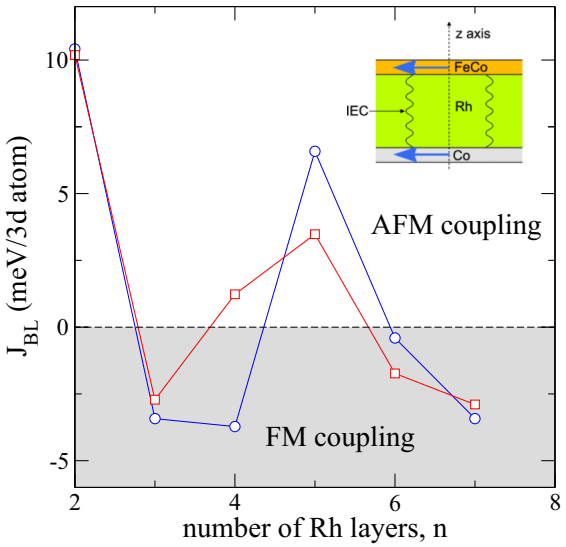

FIG. 1. (Color online) Interlayer exchange coupling in $Co/Rh_n/Co$ (circles) and $FeCo/Rh_n/Co$ (squares) magnetic films. The Rh spacers mediate an exchange coupling which couples the magnetization of the films either ferromagnetically (FM) or antiferromagnetically (AFM), depending on the spacer thickness n.

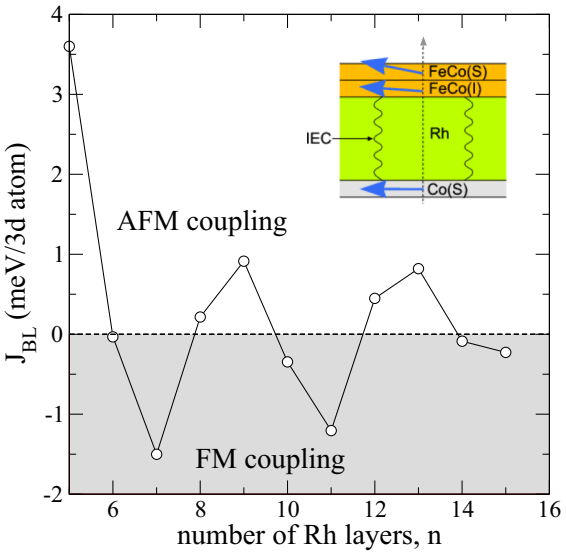

FIG. 2. (Color online) Interlayer exchange coupling in the $(FeCo)_2/Rh_n/Co$ film: the behavior is very similar to that observed for the $FeCo/Rh_n/Co$ system; in addition we show here the rather slow, oscillatory decay with increasing n.

film:

$$J_{BL} = \tfrac{1}{2}(E^{\uparrow\uparrow} - E^{\uparrow\downarrow}). \quad (6)$$

Positive values of the J_{BL} indicate that the AFM coupling is more favorable while negative values denote that the FM coupling is more favorable. For the calculations of the IEC, 78 $\mathbf{k}_\parallel$ points in the IBZ were used for $Co/Rh_n/Co$ and $FeCo/Rh_n/Co$ magnetic films and 256 $\mathbf{k}_\parallel$ points for the $(FeCo)_2/Rh_5/Co$ system. The IEC calculation is shown in Fig. 1 for $Co/Rh_n/Co$ and $FeCo/Rh_n/Co$ as a function of n. For $n = 7$, the values for J_{BL} corresponding to the Co and FeCo films are -3.4 and -2.9 meV per $3d$ atom, respectively. These values can be compared with the IEC mediated by Ag or Au spacers, where the calculated IEC for, e.g., a Fe/Ag/Fe or Fe/Au/Fe film of similar thickness is one order of magnitude smaller [34,35].

From Fig. 1 we can see clearly that the interlayer magnetic coupling oscillates with increasing Rh spacer thickness, i.e., the Rh spacers mediate an interlayer coupling which couples the magnetizations either ferromagnetically or antiferromagnetically depending on the spacer thickness. Our calculations yield a strong AFM interlayer exchange coupling for five layers of Rh and a FM coupling for seven layers, in good agreement with experimental observations for thicker magnetic films [36].

B. $(FeCo)_m/Rh_5/Co$ films

The above study refers to a collinear moment arrangement, i.e., either parallel or antiparallel to a specific direction. We consider now films with a 5-ML Rh spacer under noncollinear constraints, assuming that the magnetization direction of the Co layer is fixed in plane according to the strong in-plane anisotropy (see Table II). Since the easy axis of the FeCo is out of plane, we allow a noncollinear arrangement varying φ for this layer (see inset of Fig. 3) introducing a constraint field that stabilizes the spin configuration [26]. In this calculation, spin-orbit interaction can be conveniently included in the Hamiltonian.

The two systems $FeCo/Rh_5/Co$ and $(FeCo)_2/Rh_5/Co$ have been selected for the noncollinear calculations. In Table II, we already showed the values for the MCA for Co and FeCo layers on five- and seven-layer Rh(001) films: Among the thinner films, only the $(FeCo)_2/Rh_5/(FeCo)_2$ film has a strong perpendicular anisotropy of 0.11 meV per $3d$ atom, while Co and FeCo monolayers on five layers of Rh show an in-plane magnetization. Also, the easy axis of an antiferromagnetically coupled $FeCo/Rh_5/Co$ structure is in plane with a value of -0.36 meV per $3d$ atom. This is compatible with the average of the $Co/Rh_5/Co$ and $FeCo/Rh_5/FeCo$ results (-0.28 meV per $3d$ atom). On the other hand, the MCA in the $(FeCo)_2/Rh_5/Co$ film is dominated by the perpendicular anisotropy of the $(FeCo)_2$ layer and, in total, a positive value of 0.10 meV per $3d$ atom is obtained. This shows that the MCA values of asymmetric films cannot generally be inferred from an averaging of the symmetric ones, at least for thin spacer layers. Since the MCA is a quantity that depends sensitively on the states near the Fermi level, the different charge transfer of FeCo and Co layers and the requirement of a common Fermi level on both sides of the film can lead to substantial deviations from a simple additive model.

Comparing the IEC, we see that $(FeCo)_2/Rh_5/Co$ shows an IEC that is very similar to the FeCo monolayer system (see also Fig. 2), indicating that the coupling is an interface effect and will not be strongly influenced by the thickness of the magnetic layer.

In the following calculations, the magnetization direction of the Co layer is fixed in plane, while the direction of the FeCo double layer was varied from parallel to antiparallel alignment. The directions of the Rh moments were allowed to vary freely between the magnetic layers. The constrained SDFT results

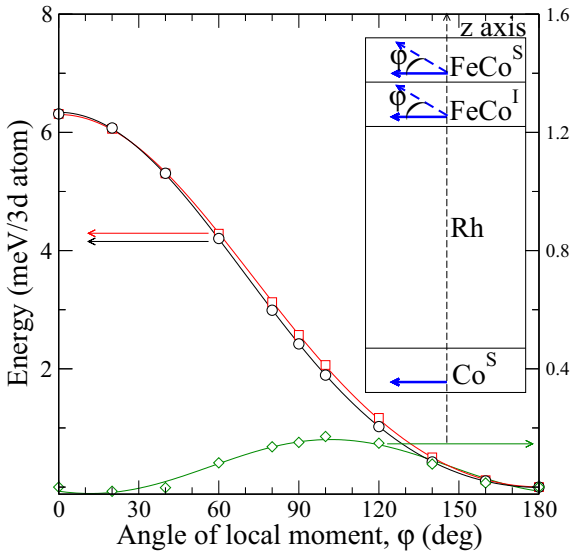

FIG. 3. (Color online) Interlayer exchange coupling with and without SOC in a $(FeCo)_2/Rh_5/Co$ magnetic film. The magnetization direction of the Co layer was fixed in plane, while the direction of the FeCo was varied from ↑↑ to ↑↓ alignment. Symbols are results from constrained SDFT; circles: E_{tot} with SOC, squares: E_{tot} without SOC. Diamonds indicate the difference of these two results E_{SOC} multiplied by −5. The full line corresponds to the fitting to Eqs. (3) and (5), in the fit to the difference (diamonds), we allow for a phase shift in the $\cos^2(\varphi)$ curve as explained in the text.

were mapped onto Eqs. (3) and (5). We found from the fitting to Eq. (3) the following parameters from scalar relativistic (SR) and SOC calculations: $J_{BL}^{SR} = 3.53$ meV/3d atom, $J_{BQ}^{SR} = 0.62$ meV/3d atom, and from Eq. (5) we get $J_{BL}^{SOC} = 3.17$ meV/3d atom and $J_{BQ}^{SOC} + K_{MCA} = 0.71$ meV/3d atom. If we assume that the bilinear and biquadratic terms are modified by SOC in a similar way, $J_{BL}^{SOC}/J_{BL}^{SR} = J_{BQ}^{SOC}/J_{BQ}^{SR}$, this leads to $J_{BQ}^{SOC} = 0.56$ meV/3d atom and $K_{MCA} = 0.15$ meV/3d atom, similar to the MCA value obtained from the symmetric bilayer film (0.11 meV).

Graphically, K_{MCA} can be extracted from the difference: $E_{tot}^{SOC} - \alpha E_{tot}^{SR} = K_{MCA}\cos^2\varphi$ where α plays the role of a rescaling factor ($\alpha = J_{BL}^{SOC}/J_{BL}^{SR} = 0.9$). The magnitude of K_{MCA} can be obtained from the difference of these fitted curves. We observe that the extrema of this difference are shifted to larger angles and its behavior is better described by a $\cos^2(\varphi - \vartheta)$ dependence with $\vartheta = 11.9°$. This shift reflects a modification of the interaction between the ordered alloy bilayer on one and the Co layer on the other side by SOC effects. Figure 3 shows the angle dependence of the energies and we obtained $K_{MCA} = 0.18$ meV per 3d atom from the fitting procedure.

For the $FeCo/Rh_5/Co$ film, similar calculations gave an in-plane magnetocrystalline anisotropy of about −0.1 meV per 3d atom for the FeCo film, which is in qualitative agreement with the value of −0.03 meV/3d atom for the symmetric $FeCo/Rh_5/FeCo$ film.

Let us now analyze these results according to the experimental results on the $Fe_{1-x}Co_x$ alloy films that have been reported in Refs. [15,17]. It was found that ultrathin films with a cobalt content between $x = 0.33$ and 0.66 show a perpendicular anisotropy, for $x = 0.6$ the magnetization remained out of plane up to a thickness of 15 layers. This behavior is in line with our calculated results for $Fe_{1-x}Co_x$ monolayers [21]. If a such a film with perpendicular anisotropy is coupled to an in-plane magnetized film by IEC, experimental evidence for a nonorthogonal magnetization was found in these layered magnetic systems [17]. Recording a depth-dependent magnetization profile through a (normally in-plane magnetized) six-layer Fe film that was exchange coupled via a Rh(001) spacer to an out-of-plane magnetized FeCo film, showed near the Rh/Fe interface strong out-of-plane components of the magnetization, which, at larger distance from the interface, turned into an in-plane magnetization [37].

We try to interpret these results inspired by the constrained SDFT results: In the case of two ferromagnetic films separated by a paramagnetic spacer layer, Bruno's coupling model predicts that the largest contribution to the IEC is due to the oscillations caused by the reflections of the electrons at the interfaces between the spacer and the magnetic layers. There are also oscillations of the IEC with the thickness of the magnetic layer, but their amplitude turned out to be much smaller than that of the oscillations with the spacer thickness. In particular, no change of sign of the IEC with the thickness of the magnetic layers has been reported [6,13]. This has been confirmed experimentally [38,39] and theoretically [40–43]. Therefore, we think that our results from ultrathin (two atomic layers) magnetic films qualitatively show the interplay between IEC, intralayer exchange coupling, and magnetic anisotropy.

The magnetization direction of the Co was fixed in plane, while the direction of the FeCo was varied and oriented to nonequilibrium directions (i.e., producing a noncollinear ordering) by a magnetic field that is the constraining field B_c in the 3d atom keeping the local magnetic moment parallel to the prescribed direction. This field is related to the energy difference between the ferromagnetic state and a state with angle φ between the magnetic moments according to [26]

$$E(\varphi) - E(\varphi = 0) = -\mu_B \sum_\nu \int_0^\varphi M_\parallel^\nu(\varphi) B_c^\nu(\varphi) d\varphi, \qquad (7)$$

where $M_\parallel^\nu$ is the component of the magnetization of atom ν parallel to the prescribed direction (φ) and the sum runs over all atoms in the magnetic layers. Thus, B_c^ν can be interpreted as a torque acting on atom ν.

Figure 4 shows that the constraint fields are large at the FeCo interface layer. In other words, this means that the $(FeCo)_2/Rh_5/Co$ system shows a strong IEC through the Rh spacer at the boundaries (interfaces) as indicated in the inset of Fig. 2. Moreover, we observe that the constraint fields are site dependent, i.e., the presence of the ordered FeCo layer on one side of the Rh(001) leads to two different constraint fields at the Co side. This is a result of the in-plane modulation of the quantum well states that mediate the IEC, leading to a larger constraint field for the Co atom directly opposite to the Fe atom on the other side. The magnitude of the constraint field at the FeCo surface is reduced strongly in the second (surface) layer of the FeCo film, where the perpendicular magnetic anisotropy leads even to a change in sign of B_c. It can be seen that the IEC acts mainly on the interface, while

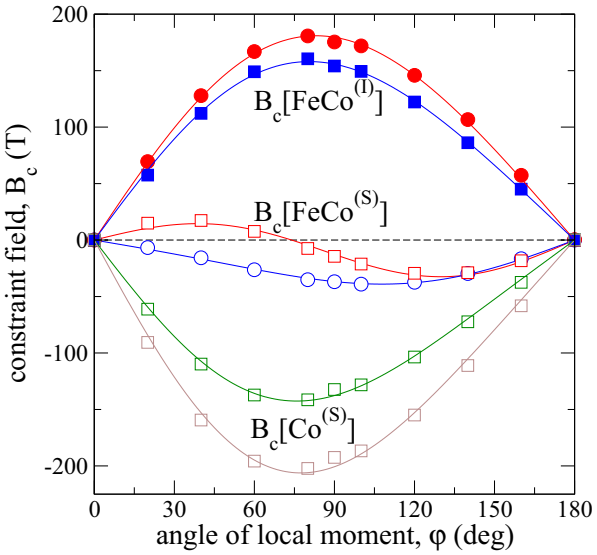

FIG. 4. (Color online) The constraint field B_c in the $(FeCo)_2/Rh_5/Co$ magnetic film. The magnetization direction of the Co layer was fixed in plane, while the direction of the FeCo was varied from 0° to 180°. Symbols are results from constrained SDFT; circles: B_c^{Fe}, squares: B_c^{Co}, full: interface (I) and open: surface (S). The solid line corresponds to the fitting with the derivative of Eq. (5) with respect to the angle φ. Due to the IEC induced by the quantum interferences in the Rh spacer, the $(FeCo)_2/Rh_5/Co$ shows a strong constraint field B_c at the FeCo interface layer. The magnitude of the B_c is reduced by about one order of magnitude at the FeCo surface layer. It can be reduced more when other layers of FeCo are added (see Fig. 5).

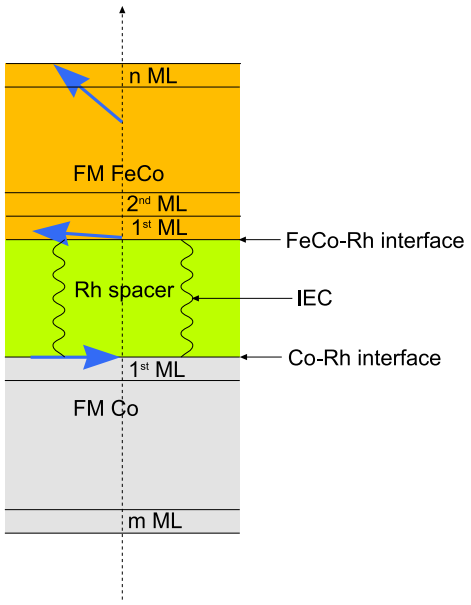

FIG. 5. (Color online) Model for the interlayer exchange coupling through a Rh(001) spacer in FeCo/Rh/Co trilayer system for a larger thickness of the magnetic films. Assuming that the intralayer exchange interaction and the in-plane anisotropy in Co are strong, we consider the magnetization direction of the Co layer as fixed. The IEC through five layers of Rh(001) mediates an antiferromagnetic coupling to the FeCo layer at the interface. As indicated by the results of Fig. 4, this interaction is only strong at the Rh interface. As the FeCo film has a strong perpendicular magnetic anisotropy, further away from the interface the magnetization tends to turn into the easy axis, leading to a noncollinear ordering within the film, unless strong intralayer exchange interaction inhibits this canting of spin directions between the layers.

contributions to the anisotropy come from all layers of the magnetic film. Therefore, only the term proportional to K_{MCA} in Eq. (5) will scale with the thickness of the magnetic film, while J_{BL} and J_{BQ} can be tuned by the spacer layer thickness (Fig. 2).

Since the IEC is rather short ranged within the magnetic film, it can be anticipated that the interplay of magnetic anisotropy and IEC leads to a noncollinearity within the magnetic layer: if the total MCA of the film can overcome the intralayer exchange coupling within the film, a layer-dependent easy axis can be expected (Fig. 5). This is in-line with the experiments on exchange-coupled layers of different anisotropy [37].

VI. SUMMARY

The IEC has been calculated for $Co/Rh_n/Co$, $FeCo/Rh_n/Co$, and $(FeCo)_2/Rh_n/Co$ films: We found an oscillatory character of the IEC with large amplitudes. The coupling energy including the spin-orbit interactions was determined for the $(FeCo)_m/Rh_5/Co$ films using constrained SDFT. Collinear calculations show an out-of-plane easy axis for $(FeCo)_2/Rh_5/Co$, while the $FeCo/Rh_5/Co$ system has an in-plane magnetic anisotropy. The MCA of the $(FeCo)_m$ side of these films was obtained by mapping the constrained SDFT results onto model Hamiltonians containing bilinear and biquadratic IEC terms and the magnetocrystalline anisotropy of the magnetically free FeCo layer. For the $(FeCo)_2$ layer, an out-of-plane easy axis is observed, indicating that in $(FeCo)_2/Rh_n/Co$ a noncollinear coupling between the Co layer and the FeCo bilayer can be realized when the bilinear IEC decreases with spacer thickness. From constrained SDFT calculations of the $(FeCo)_2/Rh_5/Co$ film, we infer that the IEC acts mainly on the magnetic layer at the interface, while the outer FeCo layer is predominantly influenced by the intralayer exchange coupling and the MCA. Due to the competition between these magnetic interactions, a noncollinear magnetic arrangement can be obtained within the FeCo film. A detailed understanding of the strength and range of magnetic interactions in such exchange coupled layers is furthermore important for the design of artificial layered magnets (e.g., Ref. [44]) that are used to realize exotic magnetic structures.

ACKNOWLEDGMENTS

Helpful discussions with D. Wortmann are gratefully acknowledged. Furthermore, S. Blizak acknowledges financial support from the Algerian ministry of higher education and scientific research. We gratefully acknowledge computing time at the JUROPA supercomputer from the Jülich Supercomputing Centre.

[1] M. B. Salamon, S. Sinha, J. J. Rhyne, J. E. Cunningham, R. W. Erwin, J. Borchers, and C. P. Flynn, Phys. Rev. Lett. **56**, 259 (1986).

[2] C. F. Majkrzak, J. W. Cable, J. Kwo, M. Hong, D. B. McWhan, Y. Yafet, J. V. Waszczak, and C. Vettier, Phys. Rev. Lett. **56**, 2700 (1986).

[3] P. Grünberg, R. Schreiber, Y. Pang, M. B. Brodsky, and H. Sowers, Phys. Rev. Lett. **57**, 2442 (1986).

[4] S. S. P. Parkin, N. More, and K. P. Roche, Phys. Rev. Lett. **64**, 2304 (1990).

[5] S. S. P. Parkin, Phys. Rev. Lett. **67**, 3598 (1991).

[6] P. Bruno, Phys. Rev. B **52**, 411 (1995).

[7] J. Mathon, M. Villeret, A. Umerski, R. B. Muniz, J. A. d'Albuquerque e Castro, and D. M. Edwards, Phys. Rev. B **56**, 11797 (1997).

[8] B. Heinrich, J. F. Cochran, M. Kowalewski, J. Kirschner, Z. Celinski, A. S. Arrott, and K. Myrtle, Phys. Rev. B **44**, 9348 (1991).

[9] M. Rührig, R. Schäfer, A. Hubert, R. Mosler, J. A. Wolf, S. Demokritov, and P. Grünberg, Phys. Status Solidi A **125**, 635 (1991).

[10] J. C. Slonczewski, J. Magn. Magn. Mater. **150**, 13 (1995).

[11] S. O. Demokritov, J. Phys. D: Appl. Phys. **31**, 925 (1998).

[12] M. D. Stiles, J. Magn. Magn. Mater. **200**, 322 (1999).

[13] P. Bruno, J. Phys.: Condens. Matter **11**, 9403 (1999).

[14] S. M. Thompson, J. Phys. D: Appl. Phys. **41**, 093001 (2008).

[15] F. Yildiz, F. Luo, C. Tieg, R. M. Abrudan, X. L. Fu, A. Winkelmann, M. Przybylski, and J. Kirschner, Phys. Rev. Lett. **100**, 037205 (2008).

[16] F. Yildiz, M. Przybylski, and J. Kirschner, J. Appl. Phys. **105**, 07C312 (2009).

[17] F. Yildiz, M. Przybylski, and J. Kirschner, Phys. Rev. Lett. **103**, 147203 (2009).

[18] P. Hohenberg and W. Kohn, Phys. Rev. **136**, B864 (1964).

[19] W. Kohn and L. J. Sham, Phys. Rev. **140**, A1133 (1965).

[20] U. Barth and L. Hedin, J. Phys. C: Solid State Phys. **5**, 1629 (1972).

[21] S. Blizak, G. Bihlmayer, and S. Blügel, Phys. Rev. B **86**, 094436 (2012).

[22] FLEUR, http://www.flapw.de/.

[23] E. Wimmer, H. Krakauer, M. Weinert, and A. J. Freeman, Phys. Rev. B **24**, 864 (1981).

[24] H. Krakauer, M. Posternak, and A. J. Freeman, Phys. Rev. B **19**, 1706 (1979).

[25] J. P. Perdew, K. Burke, and M. Ernzerhof, Phys. Rev. Lett. **77**, 3865 (1996).

[26] P. Kurz, F. Förster, L. Nordström, G. Bihlmayer, and S. Blügel, Phys. Rev. B **69**, 024415 (2004).

[27] A. R. Mackintosh and O. K. Andersen, in *Electrons at the Fermi Surface*, edited by M. Springford (Cambridge University Press, London, 1980), p. 149.

[28] C. Li, A. J. Freeman, H. J. F. Jansen, and C. L. Fu, Phys. Rev. B **42**, 5433 (1990).

[29] A. Al-Zubi, G. Bihlmayer, and S. Blügel, Phys. Rev. B **83**, 024407 (2011).

[30] P. Bruno, J. Magn. Magn. Mater. **121**, 248 (1993).

[31] P. Bruno, Phys. Rev. B **49**, 13231 (1994).

[32] R. P. Erickson, K. B. Hathaway, and J. R. Cullen, Phys. Rev. B **47**, 2626 (1993).

[33] J. C. Slonczewski, Phys. Rev. Lett. **67**, 3172 (1991).

[34] A. T. Costa Jr, J. A. d'Albuquerque e Castro, and R. B. Muniz, Phys. Rev. B **56**, 13697 (1997).

[35] J. Opitz, P. Zahn, J. Binder, and I. Mertig, J. Appl. Phys. **87**, 6588 (2000).

[36] F. Yildiz, M. Przybylski, X. D. Ma, and J. Kirschner, Phys. Rev. B **80**, 064415 (2009).

[37] J.-M. Tonnerre, M. Przybylski, M. Ragheb, F. Yildiz, H. C. N. Tolentino, L. Ortega, and J. Kirschner, Phys. Rev. B **84**, 100407 (2011).

[38] P. J. H. Bloemen, M. T. Johnson, M. T. H. van de Vorst, R. Coehoorn, J. J. de Vries, R. Jungblut, J. aan de Stegge, A. Reinders, and W. J. M. de Jonge, Phys. Rev. Lett. **72**, 764 (1994).

[39] C. H. Back, W. Weber, A. Bischof, D. Pescia, and R. Allenspach, Phys. Rev. B **52**, R13114(R) (1995).

[40] L. Nordström, P. Lang, R. Zeller, and P. H. Dederichs, Phys. Rev. B **50**, 13058 (1994).

[41] P. Lang, L. Nordström, K. Wildberger, R. Zeller, P. H. Dederichs, and T. Hoshino, Phys. Rev. B **53**, 9092 (1996).

[42] V. Drchal, J. Kudrnovský, I. Turek, and P. Weinberger, Phys. Rev. B **53**, 15036 (1996).

[43] B. Lee and Y. C. Chang, Phys. Rev. B **54**, 13034 (1996).

[44] N. S. Kiselev, C. Bran, U. Wolff, L. Schultz, A. N. Bogdanov, O. Hellwig, V. Neu, and U. K. Rößler, Phys. Rev. B **81**, 054409 (2010).